

# Compatibility Analysis for Wireless Systems in VHF/UHF Bands with Geographic Information

Kyoung-Whoan Suh, Jeong-Seok Jang, Jung-Ho Ahn

**Abstract**—By using radio propagation predictions of Rec. ITU-R P.1546 combined with geographic information, formulations for field calculation and interference analysis are presented in the VHF and UHF bands. To illustrate some computational results for the given system parameters, virtual and real geographic data are taken into account. Performance and protection ratio including the net filter discrimination are reviewed for the fixed wireless system interfered with the radar operated at the co-channel frequency as well as frequency offset. Interference effect of the victim receiver has been also examined by varying radar beam direction over azimuth and elevation angles. The developed methodology can be actually applied to evaluate interoperability between wireless systems under the net-centric warfare environment.

**Keywords**— Rec. ITU-R P.1546, interference, protection ratio, net filter discrimination, minimum coupling loss.

## I. INTRODUCTION

THE radio spectrum is a vital but limited natural resource which provides the means to convey audio, video or other information content over distances [1]. In general VHF/UHF and microwave bands are much preferred due to better propagation characteristics and are getting more spectrum utilities compared with other ones. As time goes, these trends are gradually accelerated in commercial and military applications, and each nation has a basic principle of frequency use, dividing spectrum resource into commercial and military bands [2], [3]. So the interference analysis in these bands has been greatly issued to assure interoperability or compatibility for wireless systems. Basically there are two methodologies to analyze the interference criteria. One is to use Monte Carlo Analysis-SEAMCAT (Spectrum Engineering Advanced Monte Carlo Analysis Tool), which is a statistical methodology for the simulation of random process by randomly taking values from a probability density function [4], [5]. The other is the Minimum Coupling Loss (MCL) method, which has been extensively used for estimation of interference mechanism even though it is rigid

and difficult to implement in many case not be described in static terms [6].

Recently the change in military frequency bands is reflecting 3 aspects in terms of operation, technology, and regulation [7]. The first requires higher bandwidth, greater mobility, and greater agility under a net-centric warfare (NCW). The second entails the growing spectrum requirement, caused by the advance of wireless technologies in the past 10 years and explosive demands in mobile communications, which is gradually extending encroachment to military bands. Finally regulations ask for the frequency sharing and harmonization including impacts of the World Radiocommunication Conference and host nation sovereignty [8].

Along with these trends, nowadays the battlefields are migrating from an individual centric platform to the combination of various battle elements. This enables each one to share related information in real time under NCW environment. To obtain the effective frequency use and required performance, wireless systems are essentially to keep interoperability throughout terrestrial, space, satellite, and sense networks. Thus the basic guidance of frequency utility with the exclusive assignment or independent re-use in the time or space domain can be applied to achieve those goals [9], [10]. However, to assure interoperability for various systems under NCW environment, with constraint in limited military spectra, in advance, it is necessary to study coexistence or compatibility analysis for the battlefield scenarios. Recent many studies in civil applications were presented in terms of coexistence or sharing between two different services from radio relay, fixed satellite, fixed wireless access, WiMAX, airborne radar systems [2], [11]-[17].

In addition, to calculate the radio coverage of terrestrial wireless network, commercial tools were shown based on various mathematical radio propagation models [18]-[20]. Recently to improve existing models in view of price and limited functionalities of the existing professional network planning tools, a radio signal coverage prediction software tool was developed for open-source geographical resource [21]. On the contrary, interference studies with geographic information in military bands are rarely presented due to military specialty. Thus the methodology of interference analysis combined with geographic information is essential to keep interoperability for systems operating at the VHF/UHF bands where the density of spectrum utility is getting higher and higher [7].

In this paper, to provide one of frequency coordination tools

Manuscript received June 2, 2012; Revised version received xx yy, 2012. This work was supported in part by the Agency for Defense Development (ADD) of Korea under Research Grant.

Kyoung-Whoan Suh is with the Electronics Engineering of Kangnam University, Korea (phone: +82-31-280-3808; fax: +82-31-280-3884; e-mail: kwsuh@kangnam.ac.kr).

Jeong-Seok Jang is with the Information Engineering of Dongyang Mirae College of Korea (e-mail: chang1022@hotmail.com).

Jung-Ho Ahn is with the Computer and Media Information Engineering of Kangnam University, Korea (e-mail: junggho@kangnam.ac.kr).

in the VHF/UHF bands under NCW environment, formulations for field calculation and interference analysis are presented based on Rec. ITU-R P.1546 with geographic information. Performance and protection ratio including the net filter discrimination are examined for the fixed wireless system (FWS) interfered with the radar operated at the co-channel frequency as well as frequency offset. Also interference effect of the receiver is considered by varying radar beam direction over azimuth and elevation angles.

## II. FORMULATION OF RECEIVED SIGNAL

### A. Rec. ITU-R P.1546 and Discrimination Angle

The Recommendation ITU-R P.1546 explains a method for point-to-area radio propagation predictions for terrestrial services in the frequency range of 30 MHz to 3000 MHz [22]. It can be used for calculating field strength values over land paths, sea paths and/or mixed land-sea paths between 1.0 ~ 1000 km for effective transmitting antenna heights less than 3000 m. Fig. 1 shows the field strength versus distance curves for a frequency of 600 MHz.

The propagation curves in this Recommendation mean the electric field strength for 1 kW effective radiated power (ERP) at nominal frequencies of 100, 600, and 2000 MHz, respectively. For any other frequencies, interpolation or extrapolation of the values obtained for these nominal frequency values should be used to get field strength values by virtue of the methods given in this Recommendation.

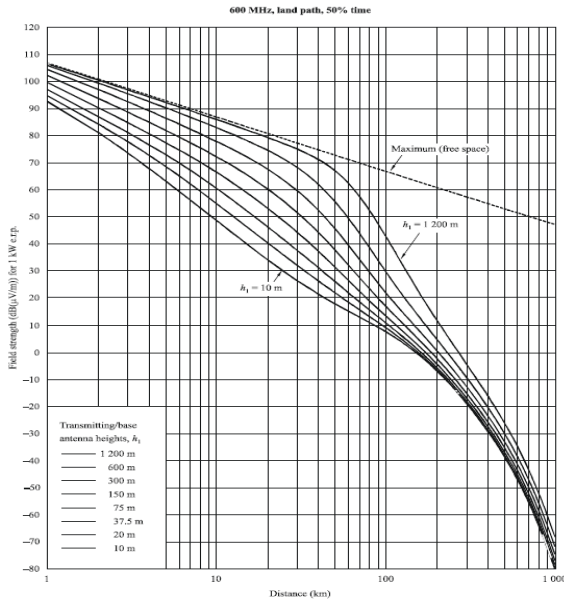


Fig. 1 Field strength versus distance curves

The received power  $P_r$  (dBm) from the Friis formula can be expressed by [23].

$$P_r = P_t + G_t + G_r - L_t - L_r - L_p \quad (1)$$

where  $P_t$  is the transmitter (Tx) power (dBm),  $G_t$  means the

Tx antenna gain in the direction of receiver (Rx) antenna (dBi),  $G_r$  is the Rx antenna gain in the direction of the Tx antenna (dBi),  $L_t$  and  $L_r$  are the total insertion loss of Tx and Rx (dB), respectively, and  $L_p$  stands for the propagation loss between Tx and Rx (dB).

Fig. 2 shows the geometry of FWS (Tx-Rx) and radar systems, where the Rx of FWS may be interfered with the radar. Let's define two vectors,  $\vec{S}$  from Rx to Tx and  $\vec{I}$  from Rx to radar. Then from two vectors one may have a S-I plane with a unit normal vector  $\hat{a}$ , and an angle  $\theta$  between two lines can be readily calculated by the inner product of two vectors, which is given by

$$\cos \theta = \frac{\vec{S} \cdot \vec{I}}{|\vec{S}| |\vec{I}|} \quad (2)$$

$$\vec{S} = (x_s - x_{Rx})\hat{x} + (y_s - y_{Rx})\hat{y} + (z_s - z_{Rx})\hat{z} \quad (3)$$

$$\vec{I} = (x_I - x_{Rx})\hat{x} + (y_I - y_{Rx})\hat{y} + (z_I - z_{Rx})\hat{z} \quad (4)$$

where the locations of Tx, Rx, and radar are given by  $r_s(x_s, y_s, z_s)$ ,  $r_{Rx}(x_{Rx}, y_{Rx}, z_{Rx})$ , and  $r_I(x_I, y_I, z_I)$ , respectively, and  $\hat{x}$ ,  $\hat{y}$ , and  $\hat{z}$  denote the unit vectors in rectangular coordinate systems. Information of each location entails geographic information of latitude, longitude, and altitude, and the distance between two systems can be easily obtained from the magnitude of each vector.

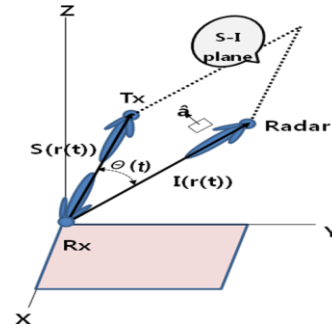


Fig. 2 Geometry of Tx, Rx and radar systems

Based on the Rec. ITU-R P.1546 the equivalent basic transmission loss for 1 kW ERP is given by

$$L_p = 139.3 - E_{p.1546} + 20 \log_{10} f \quad (5)$$

where  $L_p$  is the basic transmission loss (dB),  $E_{p.1546}$  means the electric field value ( $dB(\mu V/m)$ ) obtained from the curves of Fig. 1, and  $f$  is the frequency (MHz).

Considering the filtering effect of receiver selectivity for counteracting unwanted signal from radar in Fig. 2, the received interference power  $P_r$  (dBm) of Eq. (1) combined with Eq. (5)

is expressed by

$$P_r = E_{P,1546} + P_I + G_I + G_V - L_I - L_V - 20 \log_{10} f - 139.3 - NFD \quad (6)$$

where  $P_I$  is the peak power of the interfering system (dBm),  $G_I$  is the antenna gain of the interfering system in the direction of the victim receiver (dBi),  $G_V$  is the antenna gain of the victim receiver in the direction of the interfering system (dBi),  $L_I$  and  $L_V$  are the insertion losses of interfering system and victim receiver (dB), respectively, and  $NFD$  is a net filter discrimination (dB) depending upon transmitter spectrum mask and overall receiver filter characteristics.

### B. Net Filter Discrimination (NFD)

The definition of NFD is given by [24]

$$NFD = 10 \log_{10} \left[ \frac{P_c}{P_a} \right] \quad (7)$$

$$P_c = \int_0^\infty G(f) |H(f)|^2 df \quad (8)$$

$$P_a = \int_0^\infty G(f - \Delta f) |H(f)|^2 df \quad (9)$$

where  $P_c$  is the total power received after co-channel RF, IF, and baseband filtering, and  $P_a$  is the total power received after offset RF, IF, and baseband filtering. The function of  $G(f)$  and  $H(f)$  are transmitter spectrum mask and overall receiver filter response, respectively, and  $\Delta f$  denotes the frequency separation between a desired signal and an interference signal. Therefore it can be plainly expected that  $NFD$  yields 0 dB for the co-channel interference with  $\Delta f = 0$ . In order to calculate  $NFD$  numerically, a discrete form of Eq. (7) may be written by

$$NFD = 10 \log_{10} \left[ \frac{\left( \sum_{i=0}^{n-1} 10^{\frac{T_{ci} + R_{ci}}{10}} \right)}{\left( \sum_{i=0}^{n-1} 10^{\frac{T_{oi} + R_{ci}}{10}} \right)} \right] \quad (10)$$

where  $n$  denotes number of samples,  $|H(f)|^2 = R_{ci}(\text{dB})$  is the receiver mask sampled at a defined step frequency in co-channel,  $G(f) = T_{ci}(\text{dB})$  means the transmission mask sampled at a defined step frequency in co-channel, and  $G(f - \Delta f) = T_{oi}(\text{dB})$  is the transmission mask sampled at a defined step frequency in offset.

### C. Protection Ratio and Multiple Interferences

For the basic method of frequency coordination, a generic interference management methodology and criteria based upon the concept of a protection ratio ( $PR$ ) is adopted. It defines a minimum ratio of the relative levels of wanted to unwanted signals at the input port of the potential victim receiver for a

given link [11]. If one relates the calculated  $(C/I)_{link}$  with  $PR$  equivalent to minimum required  $(C/I)$  reflecting the maximum allowable interference, the following equation is obtained by

$$(C/I)_{link} \geq (C/I)_{\min-rqrd} (= PR) \quad (11)$$

In consequence Fig. 3 depicts the concept of  $PR$  including  $(N/I)$  and minimum required  $(C/N)$  where  $k$  is Boltzman's constant ( $1.38 \times 10^{-23} \text{ J/K}$ ),  $T$  is Kelvin temperature ( $K$ ), and  $B$  is the receiver bandwidth (Hz).

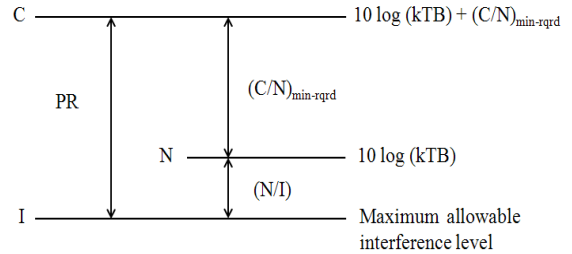


Fig. 3 Concept of protection ratio

Fig. 4 illustrates the FWS interfered with potentially multiple interferers around Rx such as  $I_1, I_2, \dots, I_n$ . Each interferer has its own position vector with respect to Rx and produces its own S-I plane from two vectors  $\vec{S}$  and  $\vec{I}_i$  as shown in Fig. 2. Then the discrimination angle  $\theta_i$  between two vectors can be obtained by the inner product, and the antenna gain for  $\theta_i$  can be found.

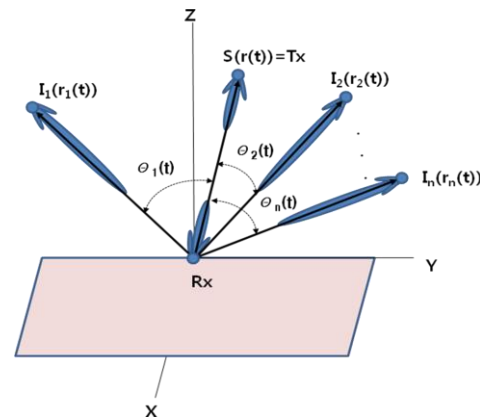


Fig. 4 Geometry of Tx-Rx and multiple interferers

The degradation of received signal caused by the Gaussian-like multiple interferers, combined with the assumed white Gaussian noise channel, is expressed by [23], [25]

$$(C/N)_i = [(N/C) + (I/C)]^{-1} \quad (12)$$

$$(I/C) = [(I_1/C) + (I_2/C) + \dots + (I_n/C)] \quad (13)$$

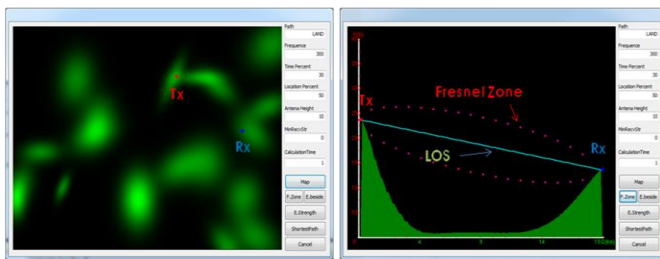
where  $(N/C)$  is the thermal noise-to-carrier ratio,  $(I/C)$  is

the equivalent interference-to-carrier ratio,  $(C/N)_t$  is the total degraded  $(C/N)$  due to multiple interferences, and  $(I_i/C)(i=1,2,\dots,n)$  is the  $i$ -th interference-to-carrier ratio.

### III. SIMULATION AND DISCUSSION

#### A. Virtual Geographic Information and Field Calculation

To illustrate the procedure for interference calculation from the derived formulations, geographic information of latitude, longitude, and altitude was generated virtually from the combinations of 10 different Gaussian functions. The area in Fig. 5-(a) is equal to  $54 \times 40 [km]^2$ . For arbitrary Tx-Rx locations in Fig. 5-(a), its path profile with the 1<sup>st</sup> Fresnel zone is depicted in Fig. 5-(b).



(a) Tx and Rx locations (b) Path profile  
Fig. 5 Geographic information and path profile

Fig. 6 shows the field strength values between Tx and Rx as a function of distance, obtained at a frequency of 300 MHz, receiver height of 10 m, and variability of 50 % in location and 30 % in time.

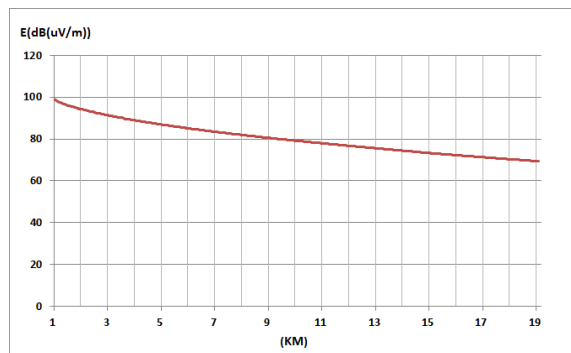


Fig. 6 Field strength values between Tx and Rx

For the sake of simplicity, it was assumed that the system parameters of FWS and radar, especially for transmitting frequency, power, and bandwidth are taken virtually to show the procedure for interference analysis. The FWS is the radio relay system used for transmitting data of STM-1 level, and its operating frequency is chosen at 2.7 GHz with occupied bandwidth of 28 MHz and channel bandwidth of 29.65 MHz. Table 1 shows the calculated protection ratio of FWS under 64-QAM and the maximum allowable  $I/N = -6.0$  dB. The required  $PR$  yields 32.3 dB which is equal to the minimum required  $C/I$  for the co-channel interference.

Table 1 FWS parameters and  $PR$

Parameters	Calculated Values	Remarks
Tx power	27 dBm	Center freq. =2.7 GHz
Ant. gain	40 dBi	$G_t = G_r$
$(C/N)_{min-reqd}$	26.3 dB @ BER $10^{-6}$	64-QAM w/o coding
$N$	-99.5 dBm	BW= 28 MHz
$C$	-73.2 dBm	
$I$	-105.5 dBm	$I/N = -6.0$ dB
$PR(=C/I)$	+32.3 dB	$NFD = 0$ dB

Next, in order to see interference effect of Rx, Fig. 7 shows BER curves as a function of  $C/I$  for FWS in Fig. 5 [26]. For the curve of  $(C/I) = \infty$  dB, it is equivalent to BER curve of  $C/N$  without interference. It is clear that from Eq. (12) BER performance is dramatically degraded as interference level increases.

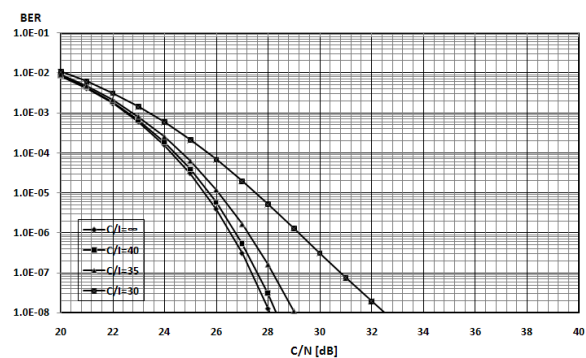


Fig. 7 BER performance for  $C/I$

In addition to examine the filtering of receiver selectivity by  $NFD$ , for instance, the curve noted by the solid line (a) in Fig. 8 was taken for a transmitter spectrum mask (dB/MHz), which can be used for FWS and radar. The curve (c) was chosen for the receiver selectivity expressed by  $|H(f)|^2 = R_{ci}(dB)$  which means the square of the overall receiver filter response [27]. The graphical concept of frequency allocations for calculating  $NFD$  are depicted in Fig. 9.

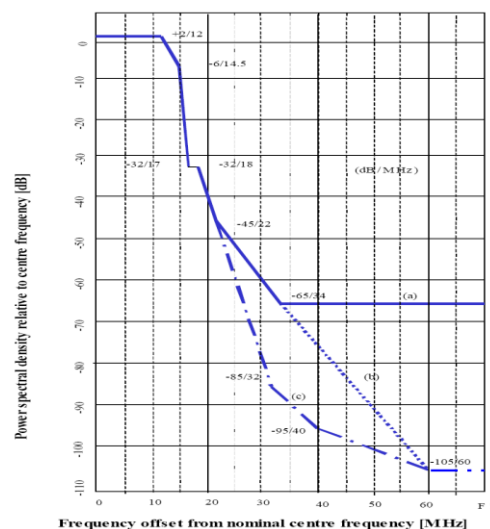


Fig. 8 Tx spectrum mask and receiver selectivity

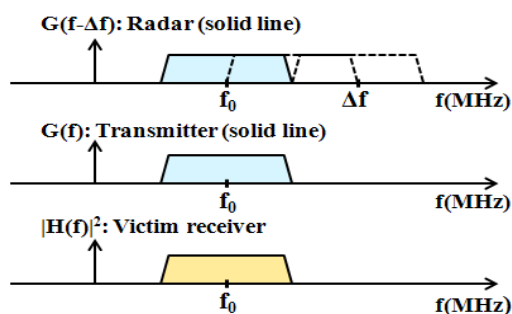


Fig. 9 Frequency allocations of FWS and radar

Fig. 10 indicates the calculated  $NFD$  as a function of frequency offset  $\Delta f$  and gives 1.9 dB and 35.9 dB at the offset of 10 MHz and 30 MHz, respectively. Even though the integral range for computing  $NFD$  is from 0 to  $\infty$  Hz, the integration was actually performed from  $f_0 - 40$  MHz to  $f_0 + 40$  MHz, where  $f_0$  is the channel center frequency, because the cumulative power beyond that bandwidth is negligible. Table 2 summarized the minimum required  $PR$  of FWS including  $NFD$  with respect to frequency offset to the channel center of FWS.

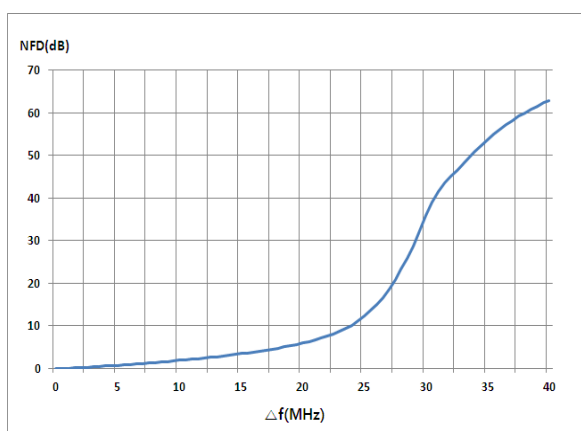


Fig. 10 Calculated  $NFD$  with frequency offset

Table 2 Required  $PR$  with frequency offset

$\Delta f$ (MHz)	$NFD$ (dB)	$PR$ (dB)
0	0	32.3
10	1.9	30.4
20	6.0	26.3
30	35.9	-3.6

On the other hand, to calculate radar interference at Rx, the case of radar interfering with Rx was considered. Table 3 illustrates the assumed parameters of radar. The centre frequency of radar and its peak power are 2.7 GHz and 40 dBm, respectively, with  $L_t = L_r = 0$  dB, and radar is operated in the range from 0 to  $\Delta f$  (MHz) regarding channel center of Rx. Also a rotationally symmetrical antenna pattern was used by Rec. ITU-R M.1652 for radar and F.699 for FWS with  $D/\lambda = 18$  where  $D$  and  $\lambda$  are the maximum size of antenna and the wavelength of frequency, respectively [28], [29].

Table 3 Radar system characteristics

Parameters	Values
Center frequency	2.7 GHz
Peak power	40 dBm (10 Watts)
Main beam gain	40 dBi ( $G_t = G_r$ )
Pulse width	0.1 $\mu$ sec
Rx IF bandwidth	28 MHz @ 3 dB
Pulse repetition rate	2000 pps
Distance from Rx	50 km
Radar altitude	About 70 m lower than Rx

Fig. 11 shows the locations of FWS and radar on the map with geographic information, where the discrimination angle between two systems can be obtained by scalar product of two vectors, resulting in  $20^\circ$  on the S-I plane. Fig. 12 depicts the path profiles for Tx-Rx and Rx-Radar, respectively.

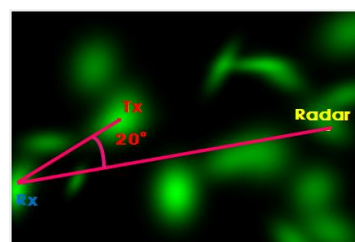


Fig. 11 Geometry of FWS and radar

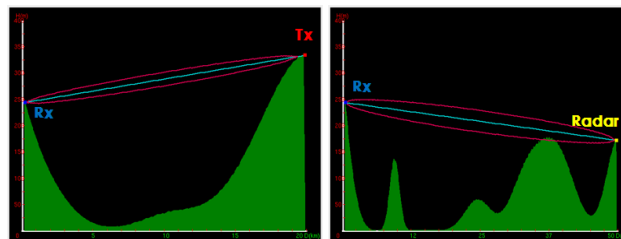


Fig. 12 Path profiles of Tx-Rx and Rx-Radar

Figs. 13 and 14 illustrate the interference power of Rx operated at the co-channel of radar. The azimuth angle  $0^\circ$  in Fig. 13 is set to the direction of radar main beam on the S-I plane in Fig. 2. It was shown that the range of azimuth angle for  $I$  less than  $-105.5$  dBm is greater than about  $7.5^\circ$ .

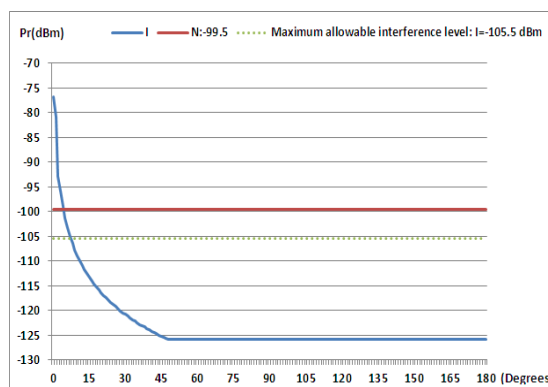


Fig. 13 Interference power of Rx in azimuth angle

In the similar way the elevation angle in Fig. 14 varies from  $-90^\circ$  to  $+90^\circ$  where the angle  $0^\circ$  is set to the direction of main beam of radar on the S-I plane. The range of elevation angle for  $I$  greater than  $-105.5$  dBm is equal to from  $-7.5^\circ$  to  $+7.5^\circ$ , which can not satisfy the required protection ratio of 32.3 dB for the given  $I/N = -6$  dB. Therefore it is concluded that for the given geometry of Fig. 11 and system parameters of Tables 1 and 3, if the off-axis angle from radar main beam is out of range from  $-7.5^\circ$  to  $+7.5^\circ$ , Rx is possible to provide the qualified performance for the given  $I/N$ . Otherwise the frequency coordination should be done inevitably by adjusting system parameters and its locations etc.

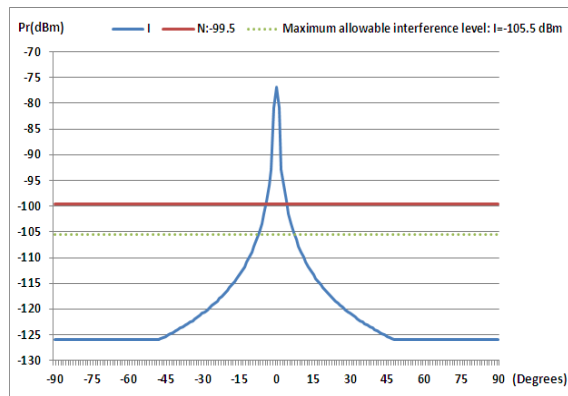


Fig. 14 Interference power of Rx in elevation angle

### B. Real Geographic Information and Interference Analysis

To show some computational results for a real map with  $80 \times 60 [km^2]$  as shown in Fig. 15, the point on the map comprises geographic information of latitude, longitude, and altitude. For arbitrary locations of Tx, Rx, and radar, path profiles with the 1<sup>st</sup> Fresnel zone are depicted in Fig. 16. And Fig. 17 illustrates the field strength values between Tx and Rx as a function of distance for 1 kW ERP, obtained at a frequency of 2700 MHz, receiver height of 10 m, and variability of 50 % in location and 30 % in time.

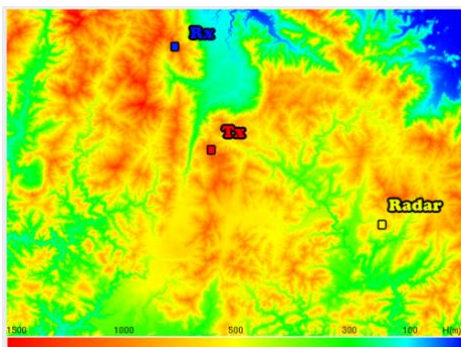
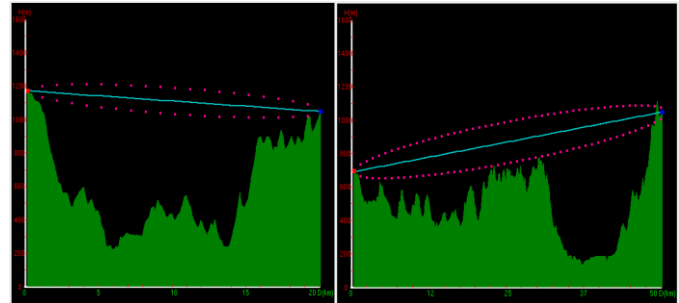


Fig. 15 Geographic information and system locations

The assumed FWS characteristics are illustrated in Table 4, which is the same as Table 1, but the channel bandwidth varied

from 28 MHz to 40 MHz. So the resultant values such as  $C$ ,  $N$ , and  $I$  were changed, but the protection ratio keeps constant because the same modulation as well as  $I/N$  level are adopted. The assumed parameters of radar are the same as Table 3 except IF bandwidth and radar altitude. The radar is operated at the co-channel FWS with 40 MHz, and the altitude of radar is 480 m lower than that of Rx.



(a) Tx-Rx (b) Radar-Rx  
Fig. 16 Path profiles of Tx-Rx and Radar-Rx



Fig. 17 Field strength values between Tx and Rx

Table 4 FWS parameters and PR

Parameters	Values	Remarks
Tx power	27 dBm	Center freq. =2.7 GHz
Ant. gain	40 dBi	$G_t = G_r$
$(C/N)_{min-rqrd}$	26.3 dB @ BER $10^{-6}$	64-QAM w/o coding
$N$	-97.98 dBm	BW=40 MHz
$C$	-71.68 dBm	
$I$	-103.98 dBm	$I/N = -6.0$ dB
$PR (=C/I)$	+32.3 dB	$NFD = 0$ dB

Now consider the calculation of interference power from Eq. (6) and two systems. The discrimination angle between Tx-Rx and Rx-Radar in Fig. 15 can be obtained by scalar product of two vectors  $\vec{S}$  and  $\vec{I}$ , resulting in about  $30.8^\circ$  on the S-I plane in Fig. 2. Fig. 18 presents the distribution of field strength  $E (dB(\mu V/m))$  around the radar in Fig. 15, which was obtained by Rec. ITU-R P.1546 under 1 kW ERP.

Next, to investigate the filtering effect of receiver selectivity by  $NFD$ , for instance, the curve noted by the solid line (a) in Fig. 19 was taken for a transmitter spectrum mask (dB/MHz), which can be used for FWS and radar, and the curve noted by the

dotted line was chosen for the receiver selectivity [30]. The calculated  $NFD$  was shown in Fig. 20 and Table 5.

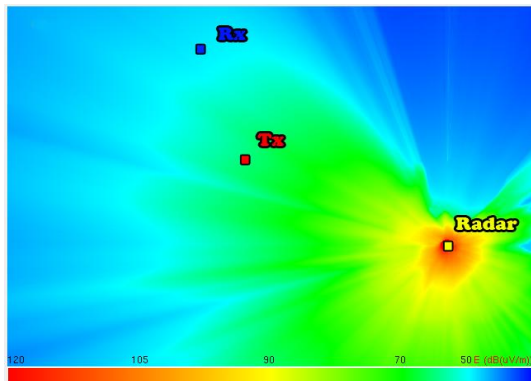


Fig. 18 Field strength distribution around radar

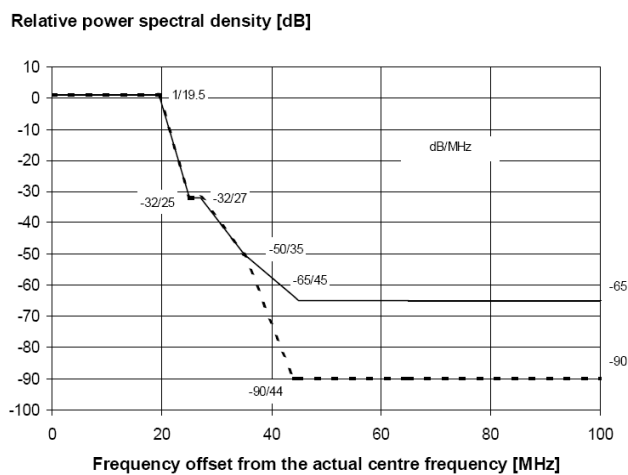


Fig. 19 Tx spectrum mask and receiver selectivity

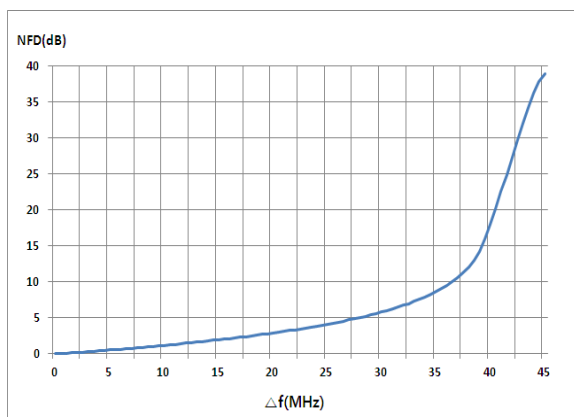


Fig. 20 Calculated  $NFD$  with frequency offset

Table 5 Required  $PR$  with frequency offset

$\Delta f$ (MHz)	$NFD$ (dB)	$PR$ (dB)
0	0	32.3
10	1.2	31.1
20	2.9	29.4
30	5.8	26.5

Finally in order to check the interference effect between two

systems for assuring interoperability, we considered the case of radar interfering with the Rx, and the rotationally symmetrical antenna patterns were adopted for both systems [28], [29].  $D/\lambda = 18$  for FWS was taken where  $D$  is the maximum size of antenna and  $\lambda$  is the wavelength of frequency.

Fig. 21 shows the interference power of Rx as functions of frequency offset and azimuth angle. Since the discrimination angle is  $30.8^\circ$ , the antenna gain of Rx can be easily determined. The azimuth angle  $0^\circ$  is set to the direction of radar main beam on the S-I plane. For the curve of frequency offset  $\Delta f = 0$  MHz, which is equivalent to co-channel operation, the received interference power is lower than the maximum allowable interference level of  $-103.98$  dBm at the azimuth angle greater than about  $5.5^\circ$ . Also for the curve of  $\Delta f = 30$  MHz, it crosses the line of the maximum allowable interference level at about  $4^\circ$ . Consequently to assure compatibility for Rx of FWS, the radar should have at least the off-axis angle greater than  $5.5^\circ$  from the main beam direction under the assumed system parameters regardless of frequency offset.

In the similar way Fig. 22 illustrates the received interference power of Rx for elevation angle and frequency offset. It is noted that all curves are symmetrical to  $0^\circ$  due to adopting the rotationally symmetric antenna pattern.

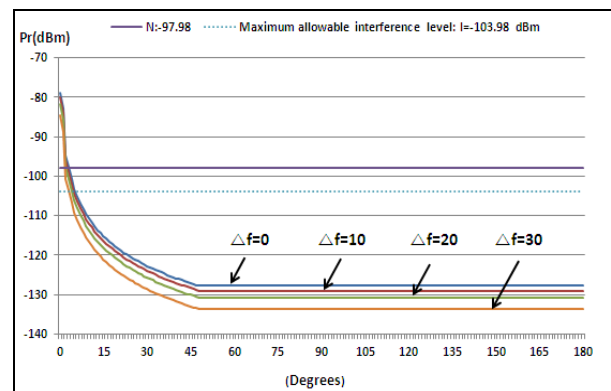


Fig. 21 Received interference power for azimuth angle

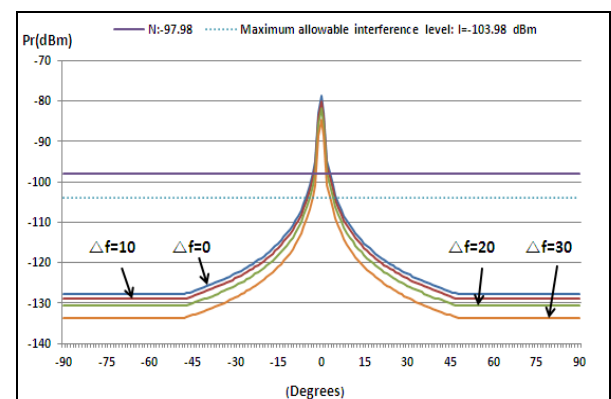


Fig. 22 Received interference power for elevation angle

#### IV. CONCLUSION

In this paper, based upon radio propagation predictions of

Rec. ITU-R P.1546 used for terrestrial services in the frequency range of 30 MHz to 3000 MHz, formulations of received signal and protection ratio have been presented to assess compatibility between wireless systems. The minimum coupling loss method was adopted for interference analysis, describing frequency-distance separation rule under the maximum allowable interference level. To illustrate some computational results for assumed system parameters, virtual and real geographic data were taken into account. Performance evaluations including protection ratio and net filter discrimination were accomplished for the fixed wireless system, interfered with the radar operating at co-channel as well as frequency offset. Moreover interference effect of the victim receiver has been also examined by varying radar beam direction with respect to azimuth and elevation angles.

The developed methodology can be actually extended to evaluate frequency coordination or compatibility for the frequency dependent systems under the net-centric warfare in the VHF and UHF bands.

#### REFERENCES

- [1] J. D. Laser and J. H. Reed, "Interference rejection in wireless communications," *IEEE Commun. Mag.*, vol. 14, May 1997, pp.37-62.
- [2] N. H. Jeong, J. H. Lee, and K. W. Suh, "Analysis of frequency sharing between mobile systems and radiolocation radars in VHF band," in *The 12th ICACT*, Korea, February 2010, pp. 1179-1183.
- [3] K. W. Suh, H. Jung, and J. H. Lee, "The calculation of field strength for DTV receiver by Rec. ITU-R P.1546," in *Proceedings of 2010 IEEE APACE*, Malaysia, November 2010 (APACE-2010-paper-ID-20).
- [4] *Monte Carlo simulation methodology for the use in sharing and compatibility studies between different radio services or systems*, Report ITU-R SM.2028-1, Switzerland 2001-2002.
- [5] *Interference protection of terrestrial mobile service systems using Monte Carlo simulation with application to frequency sharing*, Rec. ITU-R M.1634, Switzerland 2003.
- [6] *Frequency and distance separations*, Rec. ITU-R SM.337, Switzerland 1997.
- [7] K. W. Suh, J. S. Jang, J. H. Ahn, C. W. Lee, I. S. Shin, and Y. C. Jeon, "A study on interference analysis based on Rec. ITU-R P.1546 with geographic information," in *proceedings of the 1<sup>st</sup> international conference on computing, information systems and communications*, Singapore, May 2012, pp. 223-228.
- [8] ITU-R Home- <http://www.itu.int/ITU-R/>.
- [9] *Frequency and distance separations*, Rec. ITU-R SM.337, Switzerland, 1997.
- [10] *Procedure for determining the potential for interference between radar operating in the radiodetermination service and systems in other services*, Rec. ITU-R M.1461-1, Switzerland, 2003.
- [11] K. W. Suh, "A generalized formulation of the protection ratio applicable to frequency coordination in digital radio relay networks," *Radio Science*, vol. 42, RS1007, doi:10.1029/2006RS003470, 2007.
- [12] L.F. Abdulrazak, Z.A. Shamsan, and T.ABD. Rahman, "Potential penalty distance between FSS receiver and FWA for Malaysia," *WSEAS Trans. on Communications*, vol. 7, June 2008, pp. 637-646.
- [13] Z. A. Shamsan, L. Faisal, and T. A. Rahman, "On coexistence and spectrum sharing between IMT-advanced and existing fixed systems," *WSEAS Transactions on Communications*, Issue 5, Vol. 7, May 2008, pp. 505-515.
- [14] *Compatibility of services using WiMAX technology with Satellite services in the 2.3 - 2.7 GHz and 3.3 - 3.8 GHz bands*, WiMAX Forum, 2007.
- [15] Z. A. Shamsan, L. Faisal, S. K. Syed-Yusof, and T. A. Rahman, "Spectrum emission mask for coexistence between future WiMAX and existing fixed wireless access systems," *WSEAS Transactions on Communications*, Issue 6, Vol. 7, June 2008, pp. 627-636.
- [16] R. Zarookian, "Feasibility of spectrum sharing between airborne radar and wireless local area networks," M.S. thesis, Dept. Electrical Eng., Virginia Polytechnic Institute and State Univ., Blacksburg, Virginia, USA, 2007.
- [17] Suwadi, G. Hendrantoro, and Wirawan, "An area segmentation strategy for adaptive transmission to achieve near-uniform high quality coverage in 30 GHz fixed wireless cellular systems in tropical regions," *WSEAS Transactions on Communications*, Issue 8, Vol. 10, August 2011, pp. 243-253.
- [18] Planet and decibel Planner (Marconi), <http://www.ericsson.com/>.
- [19] RPS - Radio Propagation Simulator, <http://www.radiowave-propagation-simulator.de/>.
- [20] TAP-Terrain Analysis Tool, <http://www.softwright.com/>.
- [21] A. Hrovat, I. Ozimek, A. Vilhar, T. Celcer, I. Saje, and T. Javornik, "Radio coverage calculations of terrestrial wireless networks using an open-source GRASS system," *WSEAS Transactions on Communications*, Issue 10, Vol. 9, October 2010, pp. 646-657.
- [22] *Method for point-to-area predictions for terrestrial services in the frequency range 30 MHz to 3 000 MHz*, Rec. ITU-R P.1546-3, Switzerland, 2007.
- [23] R. L. Freeman, *Radio system design for telecommunication*, 2nd ed., John Wiley & Sons, Inc. 1997, pp. 695-726.
- [24] *Derivation of receiver interference parameters useful for planning fixed service point-to-point systems operating different equipment classes and/or capacities*, ETSI TR 101 854, Sophia Antipolis, France, 2005.
- [25] *Methods for determining the effect of interference on the performance and the availability of terrestrial radio-relay systems and systems in the fixed-satellite service*, Rec. ITU-R SF.766 Switzerland, 1992.
- [26] A. A. R. Townsend, *Digital line-of-sight radio links: A handbook*, Prentice Hall, Upper Saddle River, N. J., 1988, pp. 347-380.
- [27] *Fixed radio systems; point-to-point equipment; high capacity digital radio systems carrying SDH signals (up to x 2 STM-1) in frequency bands with about 30 MHz channel spacing and using co-polar arrangements or co-channel dual polarized operation*, ETSI EN 301 127, Sophia Antipolis, France, 2002.
- [28] *Dynamic frequency selection in wireless access systems including radio local area networks for the purpose of protecting the radiodetermination service in the 5 GHz band*, ITU-R M. 1652, Switzerland, 2011.
- [29] *Reference radiation patterns for fixed wireless system antennas for use in coordination studies and interference assessment in the frequency range from 100 MHz to about 70 GHz*, Rec. ITU-R F. 699, Switzerland, 2006.
- [30] *Fixed Radio Systems; Point-to-point equipment; High capacity digital radio systems carrying STM-4 in two 40 MHz channels or 2 x STM-1 in a 40 MHz channel with alternate channel arrangement*, ETSI EN 301 669 1.2.1 2001-02; Sophia Antipolis, France, 2001.

**Kyoung-Whoan Suh** was born in Gyeong-Ju, Korea, on March 16, 1960. He received the M.S. and Ph. D. degrees in Electrical and Electronic Engineering from Korea Advanced Institute of Science and Technology (KAIST) in 1988 and 1991, respectively. He is currently a professor of Electronics Engineering of Kangnam University since March 1999.

From 1991 to 1998 he was working at SAMSUNG Electronics Company as a principal engineer for developing the point-to-point and point-to-multipoint radio relay systems. His current research interests include M/W circuits and RF Modem, wireless communication system design and its performance, radio propagation and frequency coordination.

**Jeong-Seok Jang** was born in Gyeonggi-Do, Korea, on October 22, 1979. He received the M.S. and Ph. D. degrees in Radio Science and Engineering from Kwangwoon University in 2008 and 2011, respectively.

His current research interests are M/W circuits, military wireless systems, and radio propagation.

**Jung-Ho Ahn** was born in Seoul, Korea, on June 10, 1970. He received M.S. degree in Statistics from Texas A&M University and Ph.D. degree in Computer Science from Yonsei University. He is currently an assistant professor of a division of Computer and Media Information Engineering of Kangnam University since March 2007.

His current research interests include pattern recognition and computer vision algorithm such as face and gesture recognition, smart surveillance etc.